

Effect of retained chlorine in ENCAT™ 30 catalysts on the development of encapsulated Pd: insights from in situ Pd K, L₃ and Cl K-edge XAS

Mark. A. Newton, Rachel Nicholls, John B. Brazier , Bao N. Nguyen, Christopher J. Mulligan , Klaus Hellgardt , Elena M. Barreiro, Hermann Emerich, King Kuok (Mimi) Hii , Irina Snigireva & Paul B. J. Thompson

To cite this article: Mark. A. Newton, Rachel Nicholls, John B. Brazier , Bao N. Nguyen, Christopher J. Mulligan , Klaus Hellgardt , Elena M. Barreiro, Hermann Emerich, King Kuok (Mimi) Hii , Irina Snigireva & Paul B. J. Thompson (2017) Effect of retained chlorine in ENCAT™ 30 catalysts on the development of encapsulated Pd: insights from in situ Pd K, L₃ and Cl K-edge XAS, Catalysis, Structure & Reactivity, 3:4, 149-156, DOI: [10.1080/2055074X.2017.1348711](https://doi.org/10.1080/2055074X.2017.1348711)

To link to this article: <http://dx.doi.org/10.1080/2055074X.2017.1348711>



© 2017 The Author(s). Published by Informa UK Limited, trading as Taylor & Francis Group



[View supplementary material](#)



Published online: 02 Aug 2017.



[Submit your article to this journal](#)



Article views: 29



[View related articles](#)



[View Crossmark data](#)

Effect of retained chlorine in ENCAT™ 30 catalysts on the development of encapsulated Pd: insights from in situ Pd K, L₃ and Cl K-edge XAS

Mark. A. Newton^a, Rachel Nicholls^b, John B. Brazier^c , Bao N. Nguyen^b, Christopher J. Mulligan^c , Klaus Hellgardt^d , Elena M. Barreiro^c, Hermann Emerich^e, King Kuok (Mimi) Hii^c , Irina Snigireva^f and Paul B. J. Thompson^g

^aDepartment of Physics, University of Warwick, Coventry, UK; ^bSchool of Chemistry, University of Leeds, Leeds, UK; ^cDepartment of Chemistry, Imperial College London, London, UK; ^dDepartment of Chemical Engineering, Imperial College London, London, UK; ^eSwiss-Norwegian Beamlines, ESRF, Grenoble, France; ^fEuropean Synchrotron Radiation Facility, ESRF, Grenoble, France; ^gXMaS, UK-CRG, ESRF, Grenoble, France

ABSTRACT

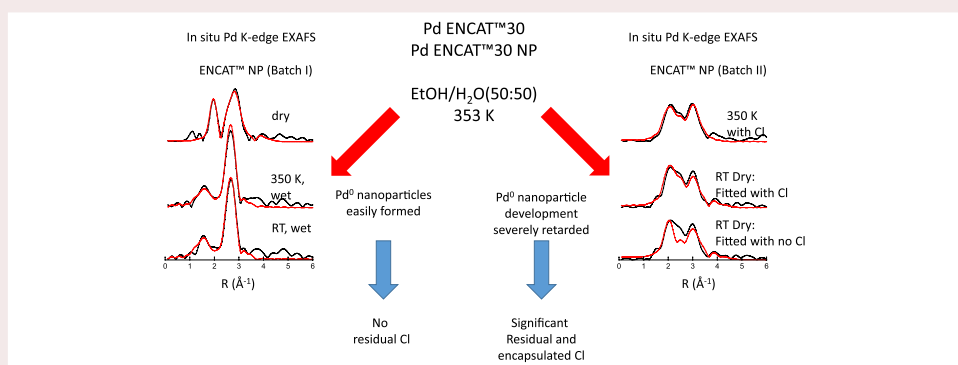
In situ X-ray absorption spectroscopy (XAS) and Pd K, L_{III}, and Cl K-edges shows that Cl can be present in significant amounts in ENCAT™ 30 catalysts and that it can severely retard Pd nanoparticle (NP) development in flowing solvents. We also show that whilst polymeric encapsulation protects the Pd against solvent induced agglomeration of Pd nanoparticles the evidence suggests it does not prevent the formation PdH_x through reaction with the aqueous ethanol solvent, and that, as received, ENCAT™ 30 NP catalysts are not, for the most part, comprised of nanoparticulate Pd⁰ irrespective of the presence of Cl.

ARTICLE HISTORY

Received 14 March 2017
Accepted 26 June 2017

KEYWORDS

Palladium; chlorine; *in situ* methods; quick EXAFS; Cl K-edge XANES; Pd L₃-edge; polymer encapsulation; green solvents; nanoparticles



1. Introduction

Selective catalysis for fine chemicals synthesis using palladium is an extremely important and much researched field. Separation of organometallic Pd catalysts from reaction products and leaching of Pd in heterogeneous Pd catalysts are two major considerations for the successful and large scale application of Pd by the pharmaceutical industry. In order to ameliorate these issues the encapsulation of either Pd organometallic species (such as palladium acetate – ENCAT™ 30- or palladium phosphines) or small palladium nanoparticles (*reduced ENCAT™ 30 = ENCAT™ 30 NP*) using polymer matrices has proved very successful [1–8], and for some years now a range of polyurea encapsulated catalysts (ENCAT™) have been commercially available and shown to be efficient and recyclable catalysts for a range of important conversions [9,10].

As part of a wider program of research using time-resolved quick scanning EXAFS (QEXAFS) to understand the fundamental behaviour of supported Pd nanoparticles in environmentally acceptable solvents, we have recently established a number of solvent induced behaviours (size dependent reducibility of PdO, formation of PdH_x species, and Pd particle growth) [11–14] that are all observed at low temperatures in mixtures of EtOH/H₂O (50:50); a solvent mixture widely employed in Pd-catalysis and highly rated in “green” solvent selection guides [15–20].

In this paper, we report the behaviour of ENCAT™ 30 catalysts under aqueous ethanol (50:50w/v) solvent flows in the temperature range 298–350 K. During our studies we observed a variability in the nature and behaviour of the Pd in these commercial catalysts which we are able to ascribe to retention of Cl that can interact with Pd in both ENCAT™ 30 (palladium acetate) and ENCAT™ 30

CONTACT Mark. A. Newton  manewton68@gmail.com, mimi.hii@imperial.ac.uk

 Supplemental data for this article can be accessed here. [<https://doi.org/10.1080/2055074X.2017.1348711>]

© 2017 The Author(s). Published by Informa UK Limited, trading as Taylor & Francis Group.

This is an Open Access article distributed under the terms of the Creative Commons Attribution License (<http://creativecommons.org/licenses/by/4.0/>), which permits unrestricted use, distribution, and reproduction in any medium, provided the original work is properly cited.

NP catalysts and affect their subsequent behaviour. We also show that, as received, ENCAT™ 30 NP is comprised mainly of Pd^{II} rather than Pd⁰. In the absence of significant Cl contamination reduced Pd nanoparticles are facilely obtained through exposure of ENCAT™ 30 NP to flowing EtOH/H₂O (50:50) at RT; however, where the catalyst is contaminated with Cl the reduction of the Pd^{II} to yield a nanoparticulate Pd is very severely retarded and essentially curtailed even at 350 K. A comparison is made between the behaviours of Cl in contact with Pd in ENCAT™ to those we have recently established for chlorinated Pd/Al₂O₃ catalysts experiencing similar conditions [14].

2. Experimental methods

2.1. Pd K-edge EXAFS

Transmission EXAFS measurements were made at the bending magnet beamlines SNBL (Swiss-Norwegian Beamlines) and BM23 at the European Synchrotron radiation facility (ESRF) using Si (1 1 1) double crystal monochromators and ion chambers for detection of X-ray absorption, normalisation, and energy scale (Pd foil) calibration. The X-ray beams (0.5 mm (V) × 2 mm (H) (B18) and 0.35 mm (V) × 3 mm (H) (SNBL)) were used to sample a 4 mm deep catalyst bed. Bi-directional Quick scanning EXAFS was employed with a time per (uni-directional) spectrum (24–25.5 keV) of between 6 and 20 s.

During experimentation QEXAFS spectra were sequentially collected along the catalyst bed at intervals of between 0.35 and 0.5 mm, starting at the inlet and ending at the outlet. This process was then repeated throughout the remainder of the experiment.

The continuous flow reactor and the overall experimental protocols followed in this study have been fully described elsewhere [11]. Briefly, the solvent used comprised 50:50 mix of H₂O/EtOH. The solvent components were individually degassed using nitrogen gas bubbled through the liquids followed by sonication after mixing. The ENCAT™ samples (ENCAT™ 30 and ENCAT™ 30 NP, 4.3 wt% Pd) were packed into a quartz tube – to yield beds of ca. 5 mm in length – and secured on either side using γ-Al₂O₃ of a smaller particle size and then quartz sand. Once loaded in the reactor the sample was located and mapped in a dry state prior to the solvent being syringe pumped through at 0.1 mL min⁻¹ flow and the bed mapped again “wet”. The sample was then heated at 1 Kmin⁻¹ under the flowing solvent to 350 K whereupon it was held at this temperature for the remainder of the experiment. Pd K-edge EXAFS maps of the bed were continually collected throughout with a single complete axial map of the bed being obtained every 5–7 min.

2.2. Cl K and Pd L₃-edge measurements

Fluorescence yield, Cl K and Pd L₃-edge measurements were made at the XMaS EPSRC UK-CRG beamline the

ESRF, Grenoble France, using a Si (1 1 1) double crystal monochromator, a Ni grid or scatter foil/Vortex Si fluorescence detector to measure the reference X-ray intensity (I_0), and a Vortex Si fluorescence detector to collect data from the samples. The latter was configured in standard fluorescence yield geometry in the horizontal plane at 9° to the incoming X-ray beam and at 45° to the sample that was held inside a purpose built chamber described in [21].

The sample (a few milligrams) was loaded into the reactor and sealed beneath a PEEK cap using 2.5 μm thick Mylar. The Mylar served to retain the samples under liquid flow (0.1 mlmin⁻¹) and provide a highly transmissive X-ray window (ca. 93–96% X-ray transmission in the energy range 2.5–3.2 keV: source [22]). This cell was mounted into a stainless steel vessel which was then maintained under a flow of He throughout all measurements.

Once loaded and mounted XAFS was collected Cl K and Pd L₃-edges prior to the introduction of the flowing liquid solvent. The sample was then measured again before being heated at 1 Kmin⁻¹ to 350 K. At 350 K the Cl K-edge and Pd L₃-edges were then measured again before the sample was cooled back to RT. A counting time per point during the XAFS scans of 10 s/point was used in all measurements.

2.3. ENCAT™ catalysts and 5 and 1 wt% Pd/Al₂O₃ catalysts

Three separate batches of ENCAT™ 30 NP along with the Pd(acetate) based ENCAT™ 30 were bought from Sigma Aldrich and used as received in all of the studies made.

The 1 and 5 wt% Pd/Al₂O₃ catalysts used for comparative purposes in this paper were prepared using PdCl₂ wet impregnation to γ-Al₂O₃ as described previously [23,24] followed by drying (air at 373 K), calcination at 773 K, and then reduction under flowing H₂ at 773 K. The as made 5wt% Pd/Al₂O₃ catalyst yielded a size distribution of particle between 2 and 4 nm in diameter in TEM (Jeol 2100F microscope) and a PdPd CN of 8 (from Pd K-edge EXAFS) after reduction in ethanol/water to 350 K. The 1 wt% Pd/Al₂O₃ reference catalyst did not yield readily observable particles in TEM and gave a PdPd CN of ca. 7 after equivalent reduction. A full description of the characterisation and behaviour of these catalysts under the same circumstances can be found in [14].

3. Results

Figure 1 shows transmission Pd K-edge EXAFS derived from two separate batches of ENCAT™ 30 NP: Batch I measured at BM23, ESRF (a); and batch II, measured at the Swiss-Norwegian beamline (SNBL), ESRF (b). In both cases the samples were measured in their “as – received” state, after they had been subjected to a flow

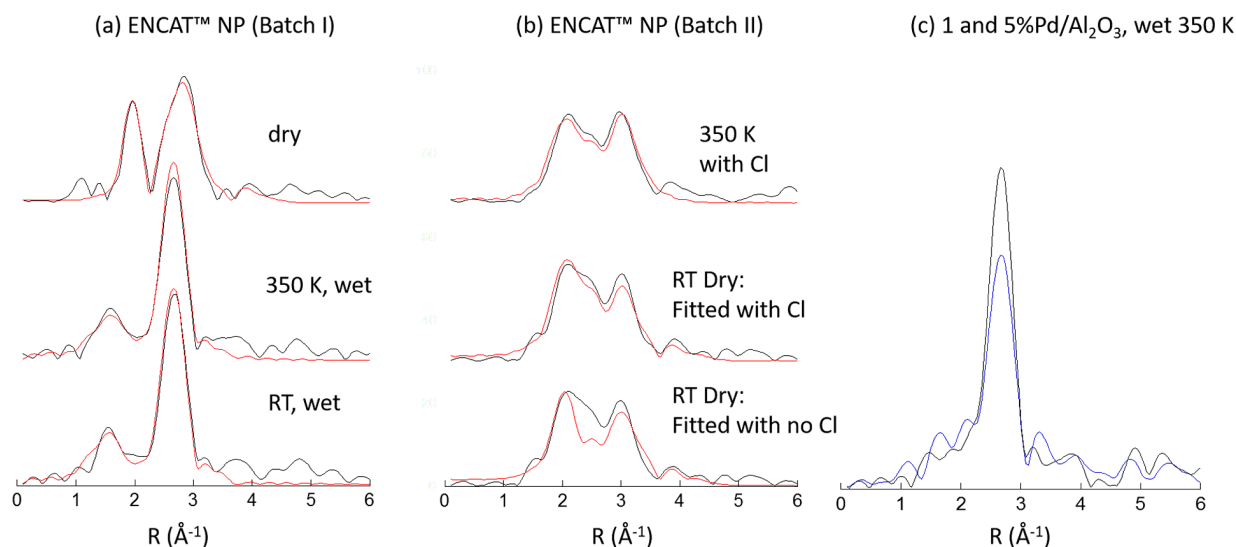


Figure 1. Comparison of Pd K-edge EXAFS (Fourier transform of k^3 -weighted data) from two batches of ENCAT™ 30 NP catalysts measured at (a) BM23 (batch I) and (b) SNBL (batch II) at the ESRF as indicated. Spectra are shown for the as received (“dry”) cases and at different states of sample evolution during heating to 350 K under an EtOH/H₂O (50:50) solvent flow. In (b) fits to the as received case are given that neglect or contain a Cl coordination to the Pd. Spectrum (c) shows Pd K-edge EXAFS derived from 1 (blue) and 5 (black) wt% Pd/Al₂O₃ catalyst after heating to 350 K under the flowing solvent mixture. In each case the ordinal axes are equivalent to aid comparison of Fourier transform intensities.

of EtOH/H₂O (50:50) at room temperature (“wet”), and again after subsequent heating to 350 K under the solvent flow. Spectrum (c) is that derived from a PdCl₂ derived 1 (blue) and 5 (black) wt% Pd/Al₂O₃ catalysts, initially comprised of nanosize PdO (2–4 nm diameter, TEM [14]), after reduction under flowing EtOH/H₂O (50:50) to 350 K. The corresponding k^3 -weighted EXAFS, along with structural and statistical information derived from analysis using EXCURV [25], for the two ENCAT™ 30 NP samples is given as supplemental data.

By comparison to the reduced Pd catalysts shown in Figure 1(c) these data clearly show that neither of the ENCAT™ 30 NP samples is initially composed of Pd nanoparticles. Some Pd–Pd scattering is observed that might be indicative of a “metallic” form of Pd, however, a coordination number (CN) of 3–3.5 is much lower than what is expected for Pd nanoparticles of the size previously reported to be present in this system (ca. 2 nm diameter) [9,10].

Using the methods derived by Benfield [26] and Jentys [27] to relate the EXAFS PdPd CN to average particle atomicity in *fcc* metals we would expect a value of ca. 9 to be returned from 2 nm diameter spherical Pd nanoparticles. The 5wt% Pd/Al₂O₃ case shows a CN of 8 is also lower than the theoretical expectation for particles of the size indicated by TEM. However, this difference can be explained by the high levels of disorder present as a result of interactions with the solvent mixture and the resultant formation of PdH_x. [12,14,28,29] The values of 3–4 for the PdPd CN exhibited in the as – received ENCAT™ 30 NP would, at best, correspond to particles of comprised of only 6–10 Pd atoms rather than the 100–200 expected from spherical particles of 2 nm diameter.

Further, in all these samples the Pd–Pd bond lengths observed, whilst consistent with a metallic Pd phase, are significantly different (Batch I = 2.73, Batch II = 2.80 and 2.76 Å for the 5 wt% Pd/Al₂O₃); and, whilst Batch I can be adequately fitted using only Pd and O scatterers, Batch II cannot. This is most clearly seen in the Fourier transform of the k^3 -weighted EXAFS data wherein an additional scatterer is required to adequately fit the EXAFS: this deficit in fitting can be removed by the addition of a Cl atom.

Upon wetting these two samples with a flow of EtOH/H₂O (50:50) and then heating to 350 K, significant differences in the reactive behaviour the two catalysts become evident. Batch I is readily transformed at RT under the flowing solvent mixture into small Pd NPs. EXAFS analysis now yields a PdPd CN of 5–6, indicating particles containing ca. 20–40 Pd atoms and average diameters of around 1 nm. The PdPd bond length returned from analysis is found to be larger (2.75 Å) than that measured concurrently from a Pd foil (2.74 Å), which we attribute again to the formation of PdH_x [12–14,28,29]. TEM [30] has previously demonstrated that, for model Al₂O₃ supported Pd nanoparticles of the size indicated to be present in the ENCAT™ 30 NP at any stage, the first shell PdPd bondlength should be substantially lower (≤ 2.7 Å). Given the experimental circumstances the most obvious source of such a discrepancy, for those catalysts exposed to the solvent mixture, is the sequestration of atomic hydrogen from the solvent by the Pd nanoparticles to yield PdH_x phase that displays considerably extended PdPd bondlengths [28,29].

In contrast Batch II remained resistant to significant changes over the period of the experiment; reduced

Pd nanoparticles are never formed to any significant degree in this case. Thus, the presence of Cl is implied to significantly affect the basic reactivity of the Pd in this system. In this case, where precious little evidence of any Pd nanoparticle formation is forthcoming, we cannot, with any confidence, assign the exceptionally long PdPd bondlengths, and the very high levels of disorder observed, to the formation of PdH_x . We may only speculate that these long PdPd bondlengths might result from the direct bonding of Cl to the very small Pd clusters and that the consistently high levels of disorder arise from a multiplicity of Pd states (except for well defined Pd nanoparticles) existing and persisting in this sample as a result.

We also note that in contrast to our previous measurements regarding conventionally supported Pd catalysts and their behaviour in the same solvent mixture [11–14], the spatially resolving component to our experimental methodology did not yield any evidence of axial gradients in Pd phase or Pd particle size along the catalyst bed.

To investigate further we then studied Batch II and two additional ENCAT catalysts (a third batch of ENCAT™ 30 NP (Batch III) and its Pd^{II} (acetate) precursor ENCAT™ 30) at the XMaS UK CRG beamline at the ESRF. This allowed us to address these systems from the perspectives of the Cl K and Pd L_3 -edges using a recently developed reactor [21] that permits the study of solids in liquid flows at X-ray energies in the 2–4 keV region whilst retaining the overall approach employed in the reactor studies made at the Pd K-edge (24.35 keV).

Figure 2 shows the Cl K-edge XANES obtained from each sample in their as-received state and, for the two ENCAT™ 30 NP samples (*batch II and batch III*), after

reaction with flowing ethanol/water (50:50) to 350 K. These are compared to the Cl K-edge XANES obtained from a PdCl_2 standard. Figure 3 then shows the corresponding Pd L_3 -edge spectra from the ENCAT™ 30 catalysts. Post-reaction spectra of the two ENCAT™ 30 NP cases are given, and again compared with spectra derived from two (1 and 5 wt% Pd as indicated) $\text{Pd}/\text{Al}_2\text{O}_3$ catalysts that have been reduced in situ under flowing $\text{EtOH}/\text{H}_2\text{O}$ (50:50) at 350 K and for which the Fourier transform have already been shown in Figure 1(c).

Firstly, it is evident that in each ENCAT™ samples studied from these perspectives a significant edge due to Cl is found. XRF measurements (see supplemental data) indicate a Pd:Cl ratio of ca. 1:1 in the ENCAT™ 30 NP cases. Furthermore, in each of these samples a clearly observable pre-edge absorption feature at ca. 2822 eV is present. Such a feature in a system such as this can only arise from Cl bonding directly to oxidised metal centres ($p \rightarrow d$ orbital mixing) [31–33]. Even in the case of the ENCAT™ 30 (Pd acetate) sample such a feature is evident with a relative intensity of ca. 0.1–0.2 compared to the PdCl_2 . Assuming that the intensity of the pre-edge feature relative to the Cl K-edge jump and to that observed in PdCl_2 is proportional to the fraction of Cl atoms that are directly bonded to oxidised Pd sites, approximately 10–20% of the Cl atoms present are implied to be directly bound to the Pd^{II} (acetate) present in the ENCAT™ 30. This fraction rises to between ca. 50–60% of the Cl binding directly to the Pd in the as received ENCAT™ 30 NP (Batches II and III).

We further observe that this feature does attenuate to varying degrees in the two ENCAT™ 30 NP samples treated in aqueous ethanol to 350 K. This would indicate

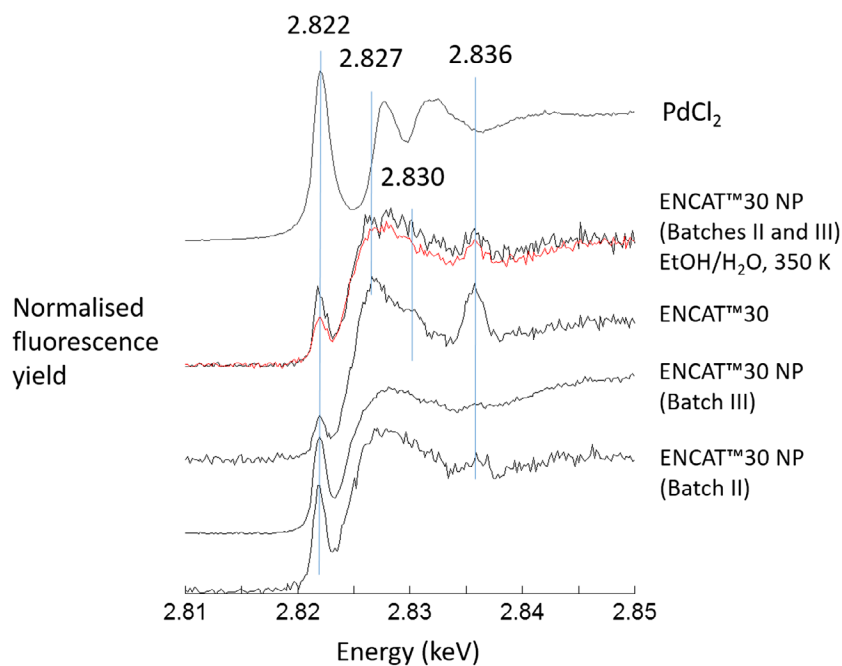


Figure 2. Cl K-edge XANES spectra derived from different ENCAT™ catalysts measured in their as received state and after reaction with flowing $\text{EtOH}/\text{H}_2\text{O}$ (50:50) at 350 K – red = Batch II, black = Batch III ENCAT™ 30 NP. The Cl K-edge XANES from a PdCl_2 standard is also given.

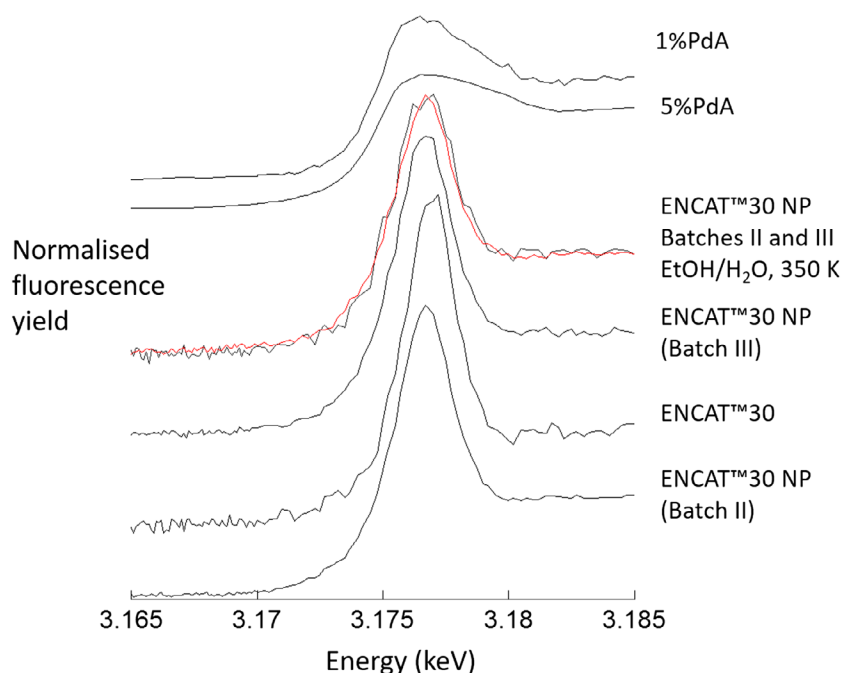


Figure 3. Pd L_3 -edge XANES derived from different ENCAT™ 30 catalysts in their as – received state and after reaction with flowing EtOH/H₂O (50:50) at 350 K – red = Batch II, black = Batch III. These are compared to two (1 and 5 wt%) Pd/Al₂O₃ catalysts, derived from a PdCl₂ precursor, measured in situ under flowing EtOH/H₂O at 350 K.

that some of this direct Cl–Pd bonding is removed by heating in the solvent mix. However, the persistence of a sizeable pre-edge feature in the Cl K-edge spectra implies that the Pd in these samples is never completely reduced to Pd⁰ under these conditions, in line with the observations from the Pd K-edge, and much Pd remain coordinated to Cl and in a non-zero oxidation state throughout.

Of further note is the presence of other, post-edge features. These are most clearly seen in the spectra of the ENCAT™ 30 sample at 2.827, 2.83, and 2.836 keV. The latter of these can also be seen to become more prominent after heating in ethanol/water to 350 K. These features correspond closely to Cl bound to Na on ClO₄, ClO₃, and ClO₂ forms, [34] implying that some of the chlorine retained is associated with residual levels of Na (arising from the use of sodium lignosulphate in polymer encapsulation process [1]) and that as a function of catalyst treatment the levels of these species can augment within the catalyst.

The Pd L_3 -edge spectra (Figure 3) then show that in each of the as received ENCAT™ samples the position and intensity of the Pd L_3 -edge white line are far more akin to that of Pd^{II} than Pd⁰ (as represented by the two spectra from the reduced Pd/Al₂O₃ samples). Whilst this is expected from the ENCAT™ 30 catalyst, it is not, a priori, expected from the ENCAT™ 30 NP cases. Congruent with both the Pd K-edge spectra (Figure 1), and the Cl K-edge data (Figure 2), the Pd L_3 -edge white line of the ENCAT™ 30 NP has only a marginally lower energy maximum and is broadened only slightly to lower binding energies, compared to ENCAT™ 30. Subsequent reaction in ethanol-water is observed to cause further reduction

of the white line intensity indicative of some level of Pd reduction occurring as a result of heating in the solvent. However, it is evident that the Pd in the two ENCAT™ 30 NP sample is never fully reduced under the conditions used here.

Figure 4 then shows derivative Pd L_3 -edge spectra for the ENCAT™ 30 (Pd acetate), the reduced 1 wt% Pd/Al₂O₃ sample and that of ENCAT™ 30 NP (Batch III) measured as received and at 350 K after reaction with aqueous ethanol. The red lines are linear combinations of the differential spectra derived from the ENCAT™ 30 (Pd acetate) and 1 wt% Pd/Al₂O₃ samples.

This exercise in quantification of the degree to which the Pd in any of these Cl containing ENCAT™ samples exists in the reduced state likely overestimates the levels of Pd⁰, given the sensitivity of the Pd⁰ XANES to particle size (Figure 3). Nevertheless, it suggests that less than 25% of the Pd is present initially as Pd⁰ and that this increases to only ca. 40% as a result of heating under the solvent mixture to 350 K. This shows a very severely retarded rate of formation of Pd NPs as compared to Batch I, wherein no evidence of Cl–Pd coordination was forthcoming from the Pd K-edge EXAFS, and reduced Pd NPs could be induced through contact with the solvent mixture at RT.

4. Discussion

The results we have obtained from three differing batches of ENCAT™ 30 NP show that a considerable variation in their composition and basic behaviour in aqueous ethanol can be observed and that, in the case of ENCAT™ 30 NP, a significant proportion of the Pd acetate has not

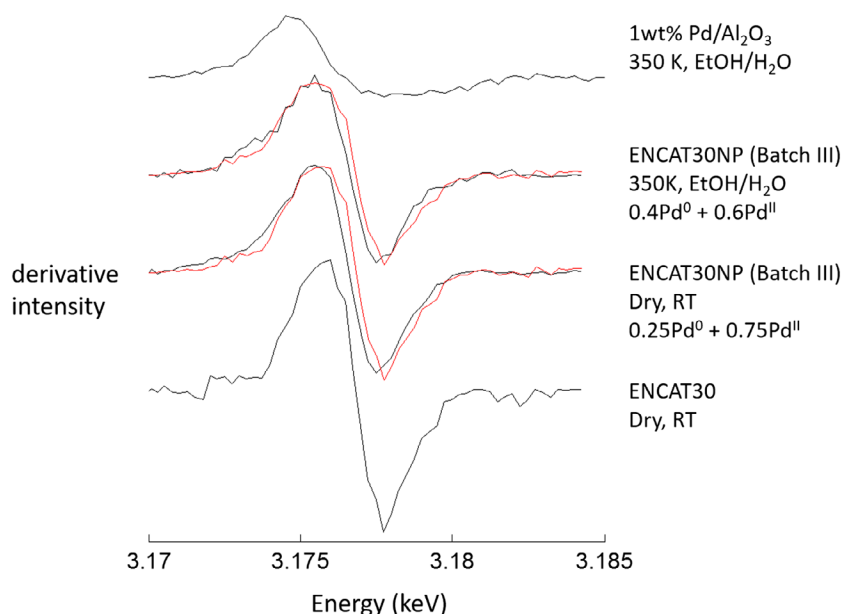


Figure 4. 1st derivative Pd L_3 -edge XANES for reduced 1 wt% Pd/Al₂O₃, as received ENCAT™ 30, and ENCAT™ 30 NP (Batch III) as received and at 350 K under flowing ethanol-water. The red lines are linear combinations of the 1 wt% Pd/Al₂O₃ (Pd⁰) as received ENCAT™ 30 (Pd^{II}) spectra in the proportions indicated.

been reduced to Pd⁰ nanoparticles during their manufacture. This observation are consistent with previous X-ray diffraction and microscopy studies of these materials [35] and we conclude that in their as received state, the majority (>75%) of Pd in the ENCAT™ 30 NP catalysts exists in a state far more akin to the Pd acetate precursor.

More importantly, however, our results show that Cl can be extensively present in ENCAT™ catalysts, and that the retention of this element can fundamentally influence the behaviour of the Pd. Two out of the three ENCAT™ 30 NP batches (batches II and III) we have investigated show significant Cl retention that results in a severe retardation of the reduction to Pd present to Pd⁰ nanoparticles. Indeed, only one batch (Batch I) of ENCAT™ 30 NP, that showed no evidence of Cl–Pd interactions, (Figure 1) was able to be facily reduced to form Pd⁰ nanoparticles at room temperature simply through exposure to the aqueous ethanolic solvent mixture.

That retained Cl in these systems leads to a very significant retardation in the reduction of Pd^{II} to Pd⁰ is in some considerable contrast to the effect of high levels of Cl in supported Pd/Al₂O₃ catalysts derived from a PdCl₂ precursor [14]. In that case, and in the limit of low Pd loading (1 wt%), the presence of retained Cl was found to significantly promote the reduction of oxidised phases of Pd present under the same conditions as used here. That the presence of Cl in the ENCAT™ catalysts has precisely the opposite effect upon the development of the Pd nanoparticles shows again that the exact role that Cl may play in the development of different types of Pd catalysts is a strong function of the nature of the Pd found initially in the catalyst.

The source of the chlorine in the ENCAT™ cases is deemed to lie in the chlorinated solvents (dichloroethane or chloroform [1–8]) used to solubilise the Pd(acetate) precursor prior to encapsulation. It seems these Cl containing species may become encapsulated with the Pd and are not reliably removed by subsequent washing procedures. EDX (see supplemental data) also shows that Na and S (from sodium lignosulfonate used in the original preparation [1]) may also be trapped and, in the former case, the Cl K-edge XANES provides evidence that this can also subsequently form NaClO_x species though reaction with some of the retained Cl.

The use of chlorinated solvents in the formation of polyurea encapsulated Pd catalysts can therefore result in extensive (to an estimated stoichiometry of PdCl, see supplemental data) retention of chlorine. In situ Pd L_3 and Cl K-edge XAS shows that a significant proportion of this chlorine interacts directly with encapsulated Pd^{II} species and can severely retard and curtail the development of fully reduced encapsulated Pd⁰ nanoparticles under the conditions used in this study. However, when Cl retention is minimal or absent Pd⁰ nanoparticles can be facily obtained at room temperature through contact with flowing ethanol/water.

Acknowledgements

BNN thank the University of Leeds for a Tenure Track Fellowship. BNN and RN thank the University of Leeds for a university research scholarship/funding. MAN is extremely grateful to the Department of Physics, University of Warwick, UK for a visiting academic position.

Disclosure statement

No potential conflict of interest was reported by the authors.

Funding

This work was supported by the EPSRC [grant number EP/G070172/1], with additional support from the Pharmacat Consortium (AstraZeneca, GlaxoSmithKline and Pfizer). EMB was supported by Xunta Galicia, and CJM is supported by an EPSRC industrial Doctoral Training Grant (AstraZeneca). JBB was funded by EPSRC "Accelerating Physical Sciences Grand Challenges towards Innovative Manufacturing": EP/L003279/1. SNBL and BM23 at the ESRF (France) are gratefully acknowledged for access to facilities.

ORCID

John B. Brazier  <http://orcid.org/0000-0001-5471-3469>

Christopher J. Mulligan  <http://orcid.org/0000-0003-1160-2202>

Klaus Hellgardt  <http://orcid.org/0000-0002-4630-1015>

King Kuok (Mimi) Hii  <http://orcid.org/0000-0002-1163-0505>

References

- Ramarao C, Ley SV, Smith SC, et al. Encapsulation of palladium in polyurea microcapsules. *Chem Commun.* 2002;10:1132–1133.
- Ley SV, Ramarao C, Gordon RS, et al. Polyurea-encapsulated palladium(II) acetate: a robust and recyclable catalyst for use in conventional and supercritical media. *Chem Commun.* 2002;10:1134–1135.
- Ley SV, Mitchell C, Pears D, et al. Recyclable polyurea-microencapsulated Pd(0) nanoparticles: an efficient catalyst for hydrogenolysis of epoxides. *Org Lett.* 2003;5:4665–4668.
- Bremeyer N, Ley SV, Ramarao C, et al. Palladium acetate in polyurea microcapsules: a recoverable and reusable catalyst for hydrogenations. *Synlett.* 2002;11:1843–1844.
- Yu JQ, Wu HC, Ramarao C, et al. Transfer hydrogenation using recyclable polyurea-encapsulated palladium: efficient and chemoselective reduction of aryl ketones. *Chem Commun.* 2003;6:678–679.
- Lee CKY, Holmes AB, Ley SV, et al. Efficient batch and continuous flow Suzuki cross-coupling reactions under mild conditions, catalysed by polyurea-encapsulated palladium (II) acetate and tetra-n-butylammonium salts. *Chem Commun.* 2005;2175–2176.
- Baxendale IR, Griffiths-Jones CM, Ley SV, et al. Microwave-assisted Suzuki coupling reactions with an encapsulated palladium catalyst for batch and continuous-flow transformations. *Chem Eur J.* 2006;12:4407–4416.
- Ley SV, Stewart-Liddon AJP, Pears D, et al. Hydrogenation of aromatic ketones, aldehydes, and epoxides with hydrogen and Pd(0)EnCat (TM) 30NP. *Beilstein J Org Chem.* 2006;2:15.
- Available from: https://www.reaxa.com/pdf/PdEncat30/Pd%20EnCat%20Flier_v3_July%2012.pdf
- Available from: https://www.reaxa.com/pdf/PdEncat30NP/Pd%20EnCat%2030NP%20Flier_v3_July%2012.pdf
- Brazier JB, Nguyen BN, Adrio LA, et al. Catalysis in flow: operando study of Pd catalyst speciation and leaching. *Catal Today.* 2014;229:95–103.
- Newton MA, Brazier JB, Barreiro EM, et al. Operando XAFS of supported Pd nanoparticles in flowing ethanol/water mixtures: implications for catalysis. *Green Chem.* 2016;18:406–411.
- Newton MA, Brazier JB, Barreiro EM, et al. Restructuring of supported Pd by green solvents: an operando quick EXAFS (QEXAFS) study and implications for the derivation of structure-function relationships in Pd catalysis. *Catal Sci Tech.* 2016;6:8525–8531.
- Brazier JB, Newton MA, Barreiro EM, et al. Effects of Cl on the reduction of supported Pd in ethanol/water solvent mixtures. *Catal, Struct React.* 2017;3:54–62.
- Capello C, Fischer U, Hungerbühler K. What is a green solvent? A comprehensive framework for the environmental assessment of solvents. *Green Chem.* 2007;9:927–934.
- Alfonsi K, Colberg J, Dunn PJ, et al. Green chemistry tools to influence a medicinal chemistry and research chemistry based organisation. *Green Chem.* 2008;10:31–36.
- Henderson RK, Jimenez-Gonzalez C, Constable DJC, et al. Expanding GSK's solvent selection guide – embedding sustainability into solvent selection starting at medicinal chemistry. *Green Chem.* 2011;13:854–862.
- Prat D, Hayler J, Wells A. A survey of solvent selection guides. *Green Chem.* 2014;16:4546–4551.
- Dunn PJ. The importance of green chemistry in process research and development. *Chem Soc Rev.* 2012;41:1452–1461.
- Prat D, Wells A, Hayler J, et al. CHEM21 selection guide of classical- and less classical-solvents. *Green Chem.* 2016;18:288–296.
- Thompson PB, Nguyen BN, Nicholls R, et al. X-ray spectroscopy for chemistry in the 2–4 keV energy regime at the XMaS beamline: ionic liquids, Rh and Pd catalysts in gas and liquid environments, and Cl contamination in gamma-Al₂O₃. *J Synchrotron Radiat.* 2015;22:1426–1439.
- Available from: https://henke.lbl.gov/optical_constants/filter2.html
- Bonivardi A, Baltanas MA. Preparation of Pd/SiO₂ catalysts for methanol synthesis 3. Exposed metal fraction and hydrogen solubility. *J Catal.* 1992;138:500–517.
- Soomro SS, Ansari FL, Chatziapostolou K, et al. Palladium leaching dependent on reaction parameters in Suzuki-Miyaura coupling reactions catalyzed by palladium supported on alumina under mild reaction conditions. *J Catal.* 2010;273:138–146.
- Binsted N. EXCURV98 CCLRC Daresbury Laboratory computer program; 1998.
- Benfield RE. Mean coordination numbers and the non-metal metal transition in clusters. *J Chem Soc Faraday Trans.* 1992;88:1107–1110.
- Jentys A. Estimation of mean size and shape of small metal particles by EXAFS. *Phys Chem Chem Phys.* 1999;1:4059–4063.
- McCaulley JA. In-situ x-ray absorption spectroscopy studies of hydride and carbide formation in supported palladium catalysts. *J Phys Chem.* 1993;97:10372–10379.
- Davis RJ, Landry SM, Horsley JA, et al. X-ray absorption study of the interaction of hydrogen with clusters of supported palladium. *Phys Rev B.* 1989;39:10580–10583.

- [30] Nepijko SA, Klimenkov M, Adelt M, et al. Structural investigation of palladium clusters on gamma-Al₂O₃(111)/NiAl(110) with transmission electron microscopy. *Langmuir*. 1999;15:5309–5313.
- [31] Shadle SE, Hedman B, Hodgson KO, et al. Ligand K-edge X-ray absorption spectroscopic studies: metal-ligand covalency in a series of transition metal tetrachlorides. *J Am Chem Soc*. 1995;117:2259–2272.
- [32] Sugiura C, Kitamura M, Muramatsu S. X-ray absorption near-edge structure of complex compounds (NH₄)₃RhCl₆, K₃RuCl₆, and Ru(NH₃)₆Cl₃. *J Chem Phys*. 1986;84:4824–4827.
- [33] Wu Y, Ellis DE. Matter, X-ray absorption near-edge spectra and electronic structure of Rhodium compounds. *J Phys Condens Mat*. 1995;7:3973–3989.
- [34] Vaudey CE, Gaillard C, Toulhoat N, et al. Chlorine speciation in nuclear graphite studied by X-ray absorption near edge structure. *J Nucl Mater*. 2011;418:16–21.
- [35] Centomo P, Zecca M, Zoleo A, et al. Cross-linked polyvinyl polymers versus polyureas as designed supported for catalytically active M⁰ nanoclusters part III. Nanometer scale structure of the cross-linked polyuria support EnCAT 30 and of the Pd^{II}/EnCat 30 and Pd⁰/EnCat 30NO catalysts. *Phys Chem Chem Phys*. 2009;11:4068–4076.